The EMBO Journal Vol.18 No.22 pp.6282–6289, 1999

Heme deficiency in erythroid lineage causes differentiation arrest and cytoplasmic iron overload

Osamu Nakajima, Satoru Takahashi, Hideo Harigae[1], Kazumichi Furuyama[1], Norio Hayashi[1], Shigeru Sassa[2] and Masayuki Yamamoto[3]

Center for Tsukuba Advanced Research Alliance and Institute of Basic Medical Sciences, University of Tsukuba, Tsukuba 305-8577, [1]Department of Biochemistry, Tohoku University School of Medicine, 2-1 Seiryocho, Aoba-ku, Sendai 980-8575, Japan and [2]Laboratory of Biochemical Hematology, The Rockefeller University, 1230 York Avenue, New York, NY 10021-6399, USA

[3]Corresponding author
e-mail: masi@tara.tsukuba.ac.jp

Erythroid 5-aminolevulinate synthase (ALAS-E) catalyzes the first step of heme biosynthesis in erythroid cells. Mutation of human ALAS-E causes the disorder X-linked sideroblastic anemia. To examine the roles of heme during hematopoiesis, we disrupted the mouse *ALAS-E* gene. ALAS-E-null embryos showed no hemoglobinized cells and died by embryonic day 11.5, indicating that ALAS-E is the principal isozyme contributing to erythroid heme biosynthesis. In the ALAS-E-null mutant embryos, erythroid differentiation was arrested, and an abnormal hematopoietic cell fraction emerged that accumulated a large amount of iron diffusely in the cytoplasm. In contrast, we found typical ring sideroblasts that accumulated iron mostly in mitochondria in adult mice chimeric for ALAS-E-null mutant cells, indicating that the mode of iron accumulation caused by the lack of ALAS-E is different in primitive and definitive erythroid cells. These results demonstrate that ALAS-E, and hence heme supply, is necessary for differentiation and iron metabolism of erythroid cells.

Keywords: ALAS-E/heme/iron metabolism/transferrin receptors/X-linked sideroblastic anemia

Introduction

5-Aminolevulinate synthase (ALAS) catalyzes the first and regulatory step of heme biosynthesis in animals (Kappas *et al.*, 1989). An erythroid-specific ALAS isozyme (ALAS-E or ALAS2) is encoded by a gene different from that which encodes the non-specific housekeeping isozyme (ALAS-N) (Yamamoto *et al.*, 1985, 1994; Riddle *et al.*, 1989). Since erythroid cells require a large quantity of heme to produce hemoglobin, this duplication of the *ALAS* gene is perhaps necessary to achieve the distinctive regulation of heme supply in erythroid and non-erythroid tissues in animals (Yamamoto *et al.*, 1994). Molecular cloning of *ALAS-E* cDNA (Yamamoto *et al.*, 1985; Riddle *et al.*, 1989) and purification of the enzyme from rat reticulocytes (Munakata *et al.*, 1993) have provided compelling evidence for the presence of ALAS-E in vertebrates. In addition, several lines of *in vitro* evidence suggest that ALAS-E is necessary for the high-level endogenous heme supply in erythroid cells (Fujita *et al.*, 1991; Lake-Bullock and Dailey, 1993; Meguro *et al.*, 1995; Harigae *et al.*, 1998). However, the *in vitro* analyses are obviously limited and do not provide a complete picture of this phenomenon *in vivo*. In particular, the contribution of ALAS-E to erythroid differentiation or cellular iron metabolism has not yet been tested rigorously *in vivo*.

The fact that the *ALAS-E* gene is localized on the X chromosome (Bishop *et al.*, 1990) led to the finding that a molecular defect in ALAS-E is responsible for X-linked sideroblastic anemia (XLSA) (Cotter *et al.*, 1992; Cox *et al.*, 1994). XLSA is characterized by X-linked hypochromic and microcytic anemia with the appearance of ring sideroblasts, i.e. erythroblasts with a large amount of mitochondrial iron deposition (Beutler, 1990). Also, translation of ALAS-E mRNA has been shown to be regulated by an iron-responsive element (IRE) in the 5′-untranslated region (UTR) of ALAS-E mRNA (Cox *et al.*, 1991; Dandekar *et al.*, 1991). These observations suggest that the expression and function of ALAS-E (i.e. erythroid heme biosynthesis) may be tightly linked to iron homeostasis (Ponka, 1997).

One approach to clarifying the roles that heme plays during erythroid differentiation is to prevent endogenous heme supply. Since heme is essential for cellular respiration in virtually every cell and animals cannot develop without heme, making animals with a complete knockout of heme biosynthesis is not technically feasible. We therefore took advantage of the fact that ALAS isozymes are encoded on separate loci. Specific disruption of the *ALAS-E* gene should make it possible to clarify the *in vivo* function of ALAS-E and its role in the high-level endogenous heme supply in erythroid cells. Therefore, we disrupted the *ALAS-E* gene in the mouse in order to examine the functional contributions of ALAS-E and the high-level endogenous heme supply to hematopoiesis and to understand the pathophysiology of XLSA.

Results

ALAS-E gene targeting

We disrupted the *ALAS-E* gene in mouse embryonic stem (ES) cells. A targeting vector was prepared that replaces a region encompassing part of exons 8 and 9 of the *ALAS-E* gene with a Neo cassette (Figure 1A). Since the head of exon 9 encodes the lysine that binds pyridoxal 5′-phosphate (PLP), an essential cofactor for ALAS activity (Gong *et al.*, 1996), a correctly targeted allele should encode a protein with null activity. The targeting construct was electroporated into ES cells, and 12 ES cell clones

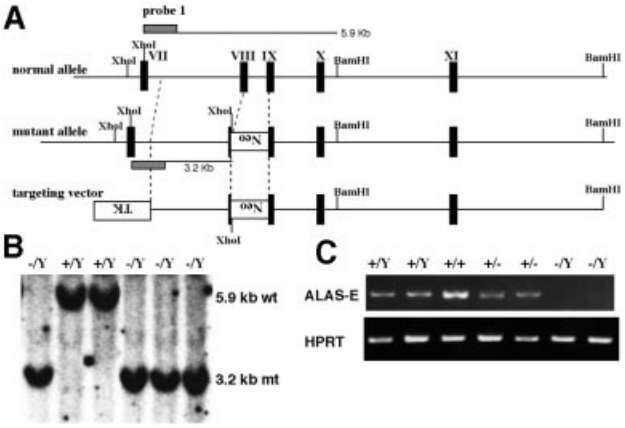

Fig. 1. *ALAS-E* gene targeting. (**A**) Structure of the *ALAS-E* gene targeting vector. The positions of the five coding exons (filled boxes) are shown in the wild-type *ALAS-E* locus (top). The targeting construct contains 3.0 kbp of genomic sequence upstream of exon 8 and 11 kbp of genomic sequence immediately downstream of the pyridoxal lysine in exon 9 (bottom). A correctly targeted allele (middle) includes a novel *Xho*I site introduced by replacement of the region from the tail of exon 8 to the head of exon 9 with a *Neo* gene cassette (Neo). TK represents the herpes simplex virus thymidine kinase gene. *Bam*HI and *Xho*I sites are shown in the figure. An 800 bp genomic region was used for Southern blot analysis (probe 1, hatched boxes). (**B**) Southern blot analysis of ES cell DNA. Genomic DNA was isolated from ES cells, digested with *Bam*HI and *Xho*I, and hybridized with probe 1. (**C**) RT–PCR analysis of ALAS-E mRNA. RNA samples from E10.0 ALAS-E mutant embryos were used as template for the RT–PCR analysis with primers specific for mouse ALAS-E. The primers amplify a 581 bp product. HPRT primers were used as an internal control.

Table I. Genotype of progeny F_1

Age	No. of litters	No. of progeny with *ALAS-E* genotype		
		+/+, +/Y	–/+	–/Y
E9.5	9	23	24	14
E10.5	3	10	12	9
E11.0	3	9	10	3
E11.5	2	5	5	4[a]
E12.5–14.5	3	17	5	0
P28	45	212	107	0
Total	65	276	163	26

[a]All pups were found to be dead.

possessing the homologously recombined allele were obtained. The genome configuration was confirmed by Southern analyses using two distinct probes, probe 1 (Figure 1B) and a Neo probe (data not shown). Finally, two independent ES cell mutations were transmitted successfully to offspring (clones 76 and 271). Since the *ALAS-E* gene is localized on the X chromosome, we first obtained heterozygous female F_1 animals with the *ALAS-E* (–/X) genotype. These heterozygous *ALAS-E* mutant females were then crossed with C57BL/6 males to prepare mutant hemizygotes (–/Y). As no male mice hemizygous for the *ALAS-E* mutation were born alive (Table I), we collected and genotyped 146 embryos ranging from embryonic day 9.5 (E9.5) to E14.5. No *ALAS-E* hemizygous mutant embryos were found viable beyond E11.5 (Table I). The absence of expression of ALAS-E mRNA in the E9.5 mutant embryos was confirmed by RT–PCR (Figure 1C).

Hemizygous ALAS-E mutant embryos are severely anemic

Whereas live ALAS-E-null mutant embryos were found up to E11.0 (Table I), these embryos were severely anemic. Blood vessels in the E10.5 yolk sac did not contain any hemoglobinized cells (Figure 2A). At E11.5, ALAS-E-null mutant embryos were completely pale and not viable (Figure 2B). These results demonstrate that ALAS-E is essential for embryonic hematopoiesis, and that without the enzyme embryos die due to the lack of primitive hematopoiesis in the yolk sac. The results also indicate that ALAS-N, the housekeeping isozyme, did not compensate for ALAS-E deficiency in the embryonic erythroid cells.

There were circulating blood cells in the E11.0 hemizygous embryos, so we stained the cells with benzidine. Whereas the majority of circulating blood cells in the E10.5 wild-type embryos stained blue with benzidine (Figure 2C), those of the ALAS-E-null mutant embryos showed no positive staining (Figure 2D). In addition, the number of circulating blood cells was markedly decreased in the mutant embryos (Figure 2D and data not shown). We also carried out immunohistochemical analysis of the primitive erythroid cells with anti-εy globin antibody (Miwa *et al.*, 1991). It was possible to detect the expression of εy globin in circulating blood cells from both wild-type and hemizygous mutant embryos (Figure 2E and F). Importantly, the content of εy globin in each ALAS-E-deficient cell appeared to be similar to that in the individual wild-type cell in this analysis. In an RT–PCR analysis, however, the level of εy globin mRNA was significantly reduced in the E10.5 mutant embryos compared with that in the wild-type embryos (data not shown), probably reflecting the reduction in the number of circulating blood cells in the ALAS-E-null mutant embryos. These findings thus indicate that in the absence of ALAS-E, primitive erythropoiesis was severely impaired.

Erythroid differentiation is arrested in ALAS-E-null mutant embryos

Blood cells collected from E10.5 yolk sacs were smeared on a slide glass and stained with Wright–Giemsa. While blood cells in the wild-type yolk sac were mature primitive erythrocytes (Figure 3A) in which nuclei occupied less than half of the cell content, hematopoietic cells in the ALAS-E-null mutant yolk sac were obviously less mature cells with large nuclei occupying the majority of the cellular space (Figure 3B). The appearance of the wild-type nuclei was rough and granular, whereas that of the mutant nuclei was fine and smooth. Flow cytometric (FACS) analysis of embryonic blood samples by forward scatter, which reflects cell size, showed that the average size of blood cells in the mutant yolk sac was larger than that in the wild-type yolk sac (Figure 3C and D). These results thus demonstrate that maturation of hematopoietic cells was arrested in ALAS-E-null mutant embryos.

To evaluate the differentiation capacity of hematopoietic progenitors in ALAS-E-null embryos, the colony-forming activity of yolk sac cells was examined. Although morphologically the colonies of wild-type and mutant yolk sac

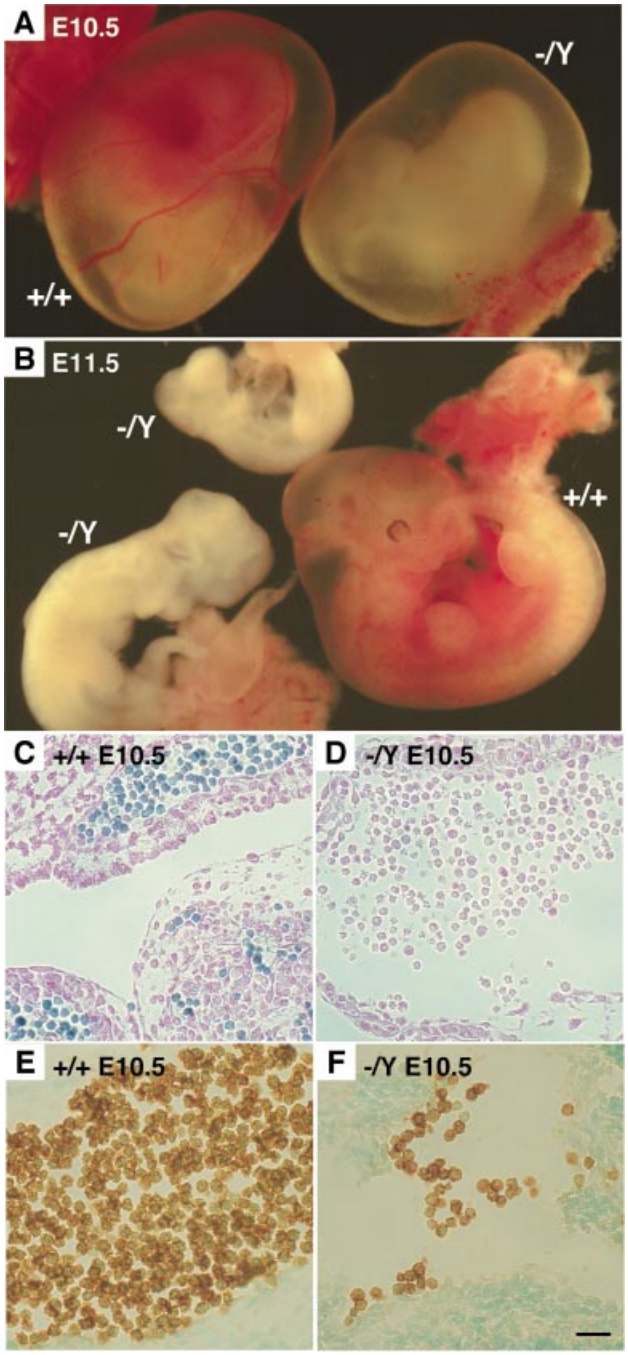

Fig. 2. ALAS-E hemizygous mutants are severely anemic. (**A** and **B**) The appearance of the ALAS-E-null mutant embryos (–/Y) and wild-type littermates (+/+) is shown at E10.5 with yolk sac (A) and at E11.5 (B). Note that the ALAS-E-null mutant embryos were alive at E10.5 but were dead and partially absorbed at E11.5. (**C** and **D**) Benzidine staining of E10.5 embryo sections. Whereas most of the primitive erythroid cells in wild-type embryos are hemoglobinized (blue) cells (C), none of the primitive erythroid cells in the ALAS-E-null mutant embryos are hemoglobinized (D). (**E** and **F**) Immunohistochemical analysis of embryonic εy globin expression in E10.5 embryos. Expression of εy globin was found in the primitive erythroid cells of both wild-type (E) and ALAS-E-null mutant (F) embryos. Scale bar, 25 μm.

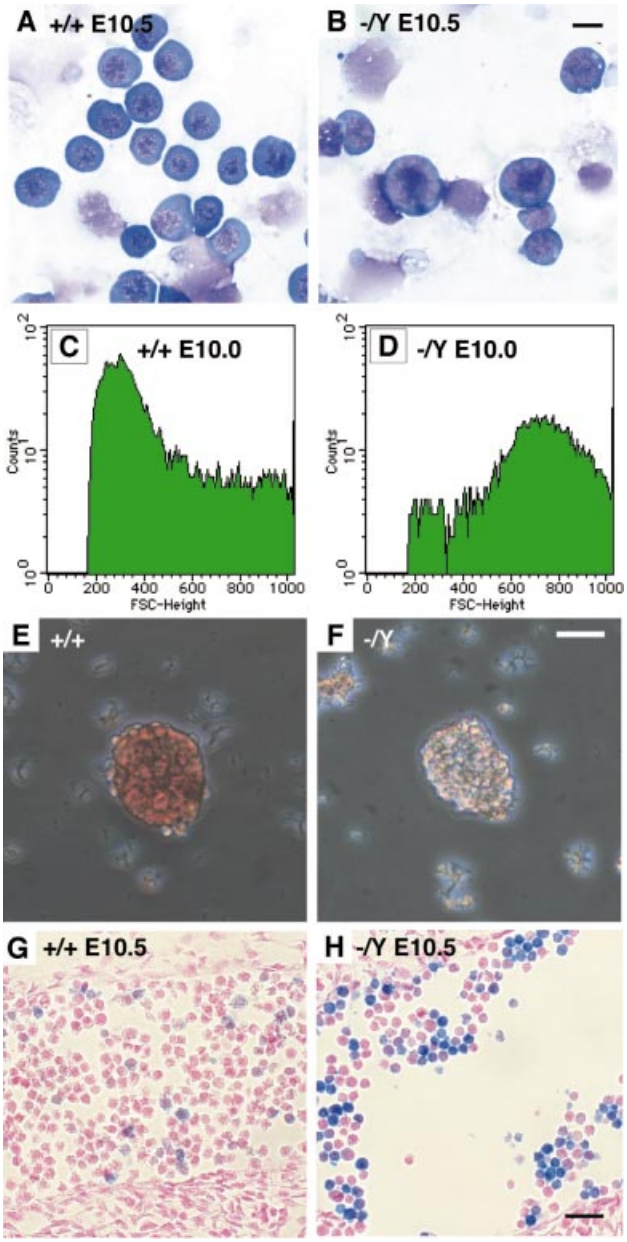

Fig. 3. Differentiation of primitive erythroid cells is arrested at the progenitor stage in ALAS-E-null mutant embryos. (**A** and **B**) The morphology of circulating blood cells in wild-type (A) and ALAS-E-null mutant (B) embryos at E10.5 was examined by Wright–Giemsa staining of blood smears. (**C** and **D**) Circulating blood cells were also analyzed by FACS. Forward scatter analysis shows that the cell size is much larger for the ALAS-E-null mutant (D) than for wild type (C). (**E** and **F**) The morphology of wild-type (E) and ALAS-E-null mutant (F) yolk sac colonies in semi-solid culture. (**G** and **H**) LacZ staining of sections from *ALAS-E (–/Y)::LacZ* mouse embryos. Note that the intensity of LacZ-positive cells in the ALAS-E-null mutant was much stronger than that of cells in the LacZ transgene embryo. Scale bars are 10 μm (A and B), 50 μm (E and F) and 25 μm (G and H), respectively.

cells appeared to be similar, hemoglobinized cells were entirely absent in the ALAS-E-null mutant colonies (Figure 3E and F). The number of colonies per 10^5 nucleated cells collected from ALAS-E-null mutant yolk sacs was approximately twice that of wild-type yolk sacs, indicating that the lack of ALAS-E did not affect yolk sac colony-forming activity (data not shown).

To investigate the timing of the arrest of primitive hematopoiesis in the ALAS-E-null mutant embryos, we took advantage of a *GATA-1* gene regulatory region–*LacZ* transgene to mark primitive erythroid cells specifically

(Onodera *et al.*, 1997). In this reporter system, the LacZ reporter is expressed far more abundantly in erythroid progenitors than in mature primitive erythrocytes. Female mice heterozygous for the *ALAS-E* mutant allele were crossed with transgenic mice homozygous for the *LacZ* transgene to generate *LacZ*-positive embryos harboring the *ALAS-E* mutation [compound mutation designated *ALAS-E (–/Y)::LacZ*]. The number of LacZ-positive blue cells detected in *ALAS-E (–/Y)::LacZ* embryos was far greater than that seen in littermates carrying only the reporter transgene. In the E9.5 embryos, LacZ-positive cells were ~29 and 76% of hematopoietic cells in the wild-type and mutant embryos, respectively (data not shown). In the E10.5 embryos, the incidence of blue cells was ~14% of that in wild-type embryos, whereas >50% of the cells were blue in the mutant embryos (compare Figure 3G and H). LacZ-positive cells in the E10.5 *ALAS-E (–/Y)* mutant embryos showed much stronger staining than the cells in wild-type embryos. The number of hematopoietic cells found in the yolk sac, aortic sac and atrial chamber of the heart was markedly decreased in the mutant embryos. Therefore, it appears that in the *ALAS-E* mutant background, primitive hematopoietic cells develop to the GATA-1-positive progenitor stage but subsequently can not differentiate into normal hemoglobinized cells (see below).

Abnormal iron accumulation in ALAS-E-null mutant erythroid cells

A molecular defect of ALAS-E is responsible for XLSA in humans, illustrating the fact that impairment of *ALAS-E* gene expression causes perturbation of iron metabolism. Indeed, histological analysis of the iron level in E9.5 and E10.5 ALAS-E-null mutant embryos showed severe accumulation of iron in the cytoplasm of circulating blood cells. The iron accumulation was observed only faintly in the E9.5 mutant embryos (Figure 4A), while it became markedly intense by E10.5 (Figure 4B). Intriguingly, unlike the scattered iron distribution pattern of ring sideroblasts (see below), which are mostly in mitochondria (Cartwright and Deiss, 1975), the pattern of iron accumulation in the *ALAS-E*-deficient erythrocytes was diffuse in the cytoplasm. We did not see this type of iron accumulation in wild-type littermates (Figure 4C). Iron thus accumulates in the mutant embryos as the primitive erythroid cells differentiate.

Another gene localized on the X-chromosome, erythroid transcription factor GATA-1, has been shown to regulate *ALAS-E* gene expression (Suwabe *et al.*, 1998). To examine whether the diffuse cytoplasmic iron accumulation can also be reproduced in *GATA-1* gene knockdown (*GATA-1.05*) (Takahashi *et al.*, 1997) hemizygous embryos, we examined iron metabolism in *GATA-1.05* embryos at E10.5. In agreement with our expectation, the lack of GATA-1 also caused diffuse cytoplasmic iron accumulation in circulating blood cells of *GATA-1.05* embryos (Figure 4D), indicating that heme deficiency in fact results in an abnormal diffuse pattern of cytoplasmic iron accumulation.

The appearance of ring sideroblasts is a hallmark of XLSA and is of critical importance for diagnosis (Furuyama *et al.*, 1997; Cotter *et al.*, 1999). Since ring sideroblasts could not be detected in the ALAS-E-null mutant embryos, we hypothesized that these cells may develop at a later stage. We therefore searched for the appearance of ring sideroblasts in the bone marrow and

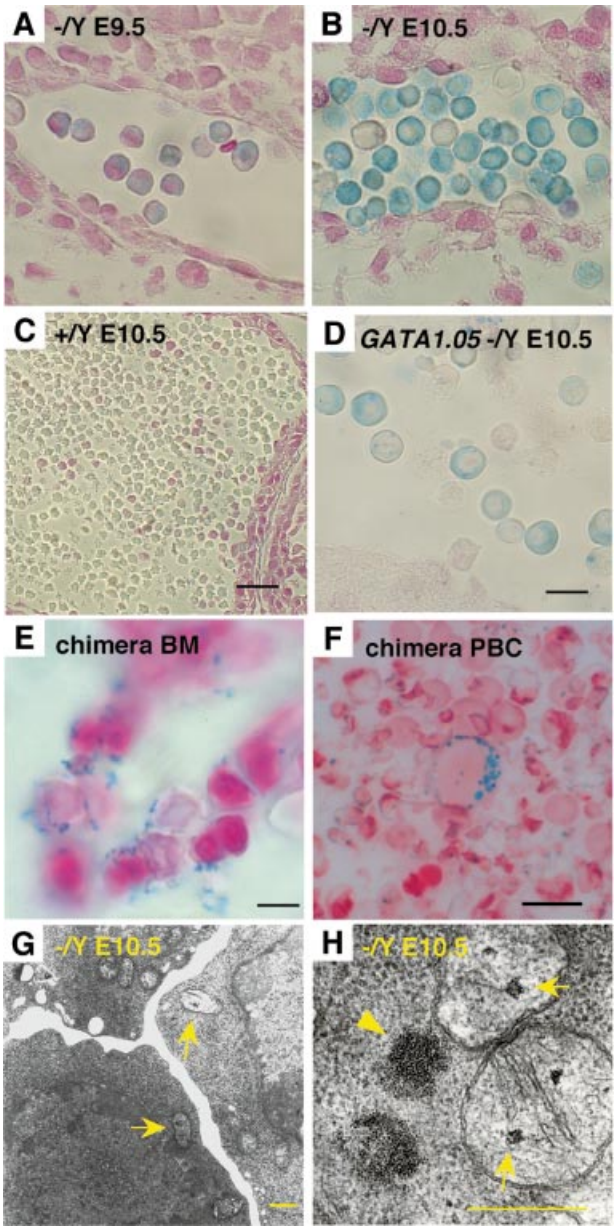

Fig. 4. Abnormal iron accumulation in the ALAS-E-null mutant erythroid cells. (A–D) Thin sections of E9.5 and E10.5 embryos were stained with Prussian Blue. While most of the circulating blood cells in the E9.5 (**A**) and E10.5 (**B**) ALAS-E-null mutant were stained blue, no such positive-staining cells were found in blood cells of wild-type embryos (**C**). Note that, while positive-staining cells show iron deposition to some extent in the mitochondria, iron accumulation in circulating blood cells of ALAS-E-null mutant embryos is mostly diffuse cytoplasmic. The intensity of the staining is much weaker in the E9.5 mutant embryo (A) than in the E10.5 mutant embryo (B). Sections from a *GATA-1.05/Y* embryo were also stained blue (**D**). (E and F) Prussian Blue staining was also carried out using bone marrow (BM, **E**) and circulating (PBC, **F**) blood cells in adult mice chimeric for ALAS-E-null and wild-type cells. The staining pattern appears to be similar to the ring sideroblasts. (**G** and **H**) Electron microscopic analysis of primitive erythroid cells was carried out using E10.5 ALAS-E-null mutant embryos. The arrows indicate mitochondrial iron deposits, whereas the arrowhead indicates a cytoplasmic ferritin aggregate. Scale bars are 10 μm (A, B and D), 25 μm (C), 5 μm (E and F) and 0.2 μm (G and H), respectively.

Table II. Iron content in E10.5 by atomic absorption spectrometry

Embryo No.	1	2	3	4	5	6
Genotype	–/Y	–/Y	+/Y	+/Y	+/Y	–/+
No. of cells ($\times 10^5$/embryo)	1.7	2.5	7.3	8.2	9.0	5.4
Iron content						
(ng/embryo)	115	155	180	170	185	160
(fg/cell)	676	620	219	207	205	296

circulating blood of adult mice chimeric for ALAS-E-null mutant and wild-type cells. Typical ring sideroblasts were found in the bone marrow (Figure 4E) and circulating blood (Figure 4F) of adult chimeric mice. Thus, the mode of iron accumulation caused by the lack of ALAS-E in definitive erythroid cells is distinct from that in primitive erythroid cells.

The diffuse cytoplasmic iron accumulation observed in the ALAS-E-deficient embryos has not been described. By electron microscopic analyses, ring sideroblasts in XLSA patients were shown to accumulate large amounts of iron in the mitochondria (see Bessis and Breton-Gorius, 1962; Bessis and Jensen, 1965). In contrast, our electron microscopic analysis revealed that mitochondrial iron deposition was not so significant in blood cells of the ALAS-E-null mutant embryo (Figure 4G and H). While arrows in Figure 4G and H show slight iron overloading in mitochondria, this profile is completely different from the image of ring sideroblasts reported in XLSA (Bessis and Breton-Gorius, 1962; Bessis and Jensen, 1965). Similarly, although cytoplasmic ferritin aggregates were found in the primitive erythroid cells (arrowhead, Figure 4H), these ferritin aggregates were atypical, in that no ferritin crystal lattice or siderosome was found in the ALAS-E-null mutant erythroid cells. Immunohistochemical analysis with anti-ferritin antibody showed that the expression level of ferritin was not increased in the ALAS-E-null yolk sac cells compared with wild-type cells (data not shown). Thus the mechanism by which cytoplasmic iron accumulated in the mutant embryos remains to be elucidated.

We then analyzed the iron accumulation quantitatively by atomic absorption spectrometry. A litter of E10.5 ALAS-E-mutant embryos was genotyped, and hematopoietic cells were dispersed from the embryos and collected. As shown in Table II, the total iron content per cell in the ALAS-E-null embryos (Nos 1 and 2) was approximately three times more than in the wild-type embryos (Nos 3–5). Similarly, the heterozygous mutant embryo (No. 6) showed a slight increase. Since the number of hematopoietic cells decreased significantly in ALAS-E-null embryos, total iron content per embryo was not increased in the mutant embryos relative to the wild-type embryos. These results thus indicate that heme deficiency caused an abnormal increase of the iron uptake, through which iron accumulated diffusely in the cytoplasm of ALAS-E-null primitive erythroid cells.

Down-regulation of transferrin receptor expression in ALAS-E-null cells

Iron available for erythroid cells is supplied mainly by the transferrin–transferrin receptor (TfR) pathway (Ponka,

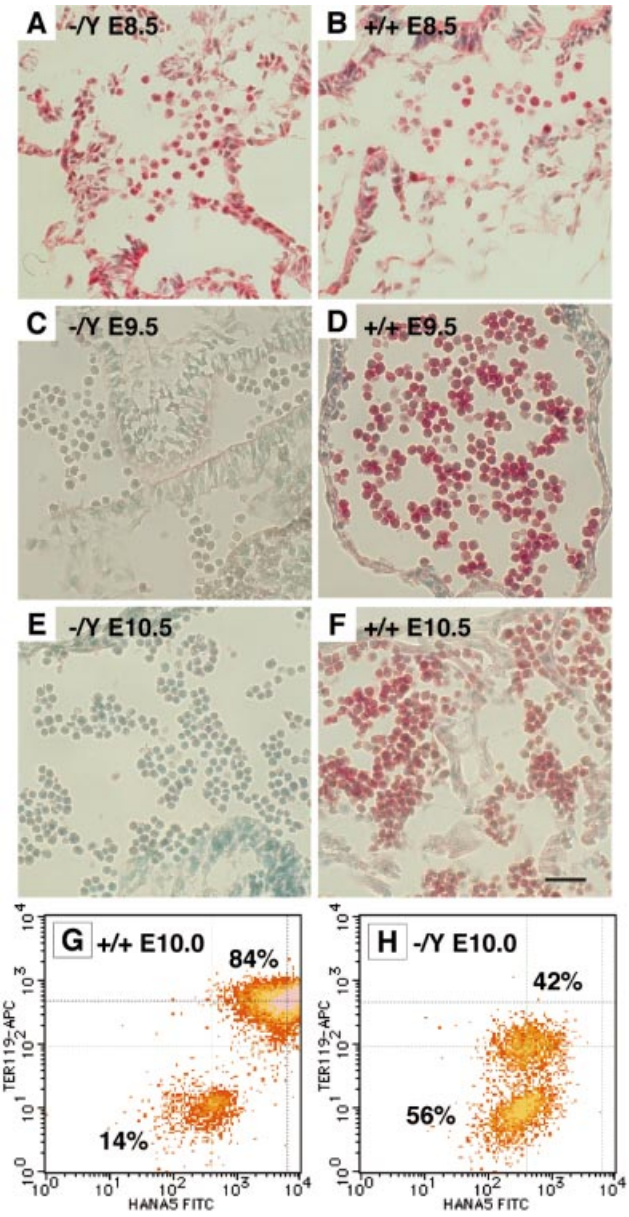

Fig. 5. TfR expression in circulating blood cells in ALAS-E-null mutant embryos. (A–F) ALAS-E-null mutant (**A**, **C** and **E**) and wild-type (**B**, **D** and **F**) embryos at E8.5 (A and B), E9.5 (C and D) and E10.5 (E and F) were examined using HANA5 antibody, which is specific for mouse TfR. (G and H) Primitive blood cells in wild-type (**G**) and ALAS-E-null mutant (**H**) embryos at E10.0 were analyzed by FACS. Note that the $TfR^{H}TER119^{H}$ population disappeared and a new $TfR^{L}TER119^{M}$ cell fraction emerged in the ALAS-E-null mutant embryo. Scale bar, 25 μm.

1997). To examine the system of iron import into the cytoplasm, we examined TfR expression immunohistochemically in ALAS-E-deficient embryos using anti-TfR antibody. TfR was expressed abundantly in both ALAS-E-null mutant and wild-type E8.5 embryos, and the expression was found not only in hematopoietic cells but also in other tissues (Figure 5A and B). Unexpectedly, however, we could not detect any TfR expression in E9.5 and E10.5 hematopoietic cells of the ALAS-E-null mutant embryos (Figure 5C and E), while TfR was highly expressed in the circulating blood cells of wild-type littermates (Figure 5D and F). In an RT–PCR analysis,

TfR mRNA expression was also markedly suppressed in the ALAS-E-null mutant E9.5 and E10.5 embryos (data not shown). An important observation here is that although the TfR level was very low in the E9.5 and E10.5 cells, cytoplasmic iron accumulated markedly during the E9.5–E10.5 stage (see Figure 4A and B). This fact suggests that cytoplasmic iron accumulation is independent of the TfR level in primitive erythroid cells.

The expression of TfR and the TER119 erythroid-specific antigen on the surface of yolk sac hematopoietic cells was examined using an FACS double sorting strategy. In the E10.0 wild-type embryo (Figure 5G), the yolk sac hematopoietic cells were found to be divided into two groups. One group (14%) of cells expressed low level TfR and TER119 ($TfR^{L}TER119^{L}$), while cells in the other group (84%) expressed TfR and TER119 at a high level ($TfR^{H}TER119^{H}$). Since TER119 is expressed exclusively only in late-stage erythroid cells including mature erythrocytes, but not in erythroid progenitors such as BFU-e or CFU-e in definitive erythropoiesis (Ikuta *et al.*, 1990), the $TfR^{H}TER119^{H}$ and $TfR^{L}TER119^{L}$ cells may correspond to primitive mature primitive erythrocytes and their progenitors, respectively.

In the E10.0 (–/Y) mutant embryos (Figure 5H), circulating blood cells were composed of $TfR^{L}TER119^{L}$ cells (56%) and cells expressing a moderate level of TER119 ($TfR^{L}TER119^{M}$, 42%). The $TfR^{L}TER119^{M}$ population was newly emerged in the ALAS-E-null mutant embryos, while the mature erythroid cell fraction was absent in the mutant embryos. The appearance of $TfR^{L}TER119^{M}$ and disappearance of $TfR^{H}TER119^{H}$ cell fractions should be attributed to the lack of ALAS-E, suggesting that ALAS-E, hence high-level endogenous heme supply, is required for the normal maturation of primitive erythroid cells. In the FACS analysis, the expression of TfR in the $TfR^{H}TER119^{H}$ wild-type cells was >12 times higher than in the $TfR^{L}TER119^{M}$ cells of the E10.0 ALAS-E-null mutant embryos. Importantly, while TfR expression was low, iron accumulated significantly in the primitive erythroid cells of the ALAS-E-null mutant embryos. This observation again suggests that the import pathway responsible for cytoplasmic iron accumulation is independent of the TfR-mediated iron transport system.

Discussion

Of the heme biosynthetic enzymes in animals, only ALAS is known to occur as tissue-specific isozymes encoded by two separate genes (Yamamoto *et al.*, 1994). This enabled us to target the *ALAS-E* gene and examine the specific contribution of heme to the erythroid differentiation process. Morphologically immature cells that show a unique $TfR^{L}TER119^{M}$ profile accumulated in the ALAS-E-null mutant embryos. Whereas the number of primitive erythroid cells was significantly lower in the *ALAS-E*-null mutant embryos (Table II), similar numbers of colony-forming cells existed in both the mutant and wild-type embryos. Thus, our results unequivocally demonstrated that the lack of ALAS-E, with its resultant low-level endogenous heme supply, causes maturation arrest of primitive erythroid cells.

We previously observed maturation arrest of primitive erythroid cells in *GATA-1.05* GATA-1 knockdown embryos (Takahashi *et al.*, 1997). The present *ALAS-E* mutant phenotype resembles, although not entirely, that observed in the *GATA-1.05* mutant embryos. Both the ALAS-E expression level and the porphyrin content were significantly reduced in erythroid cells of the *GATA-1.05* mutant mice, suggesting that *ALAS-E* is an important GATA-1 gene target (Suwabe *et al.*, 1998). However, while εy globin was not detected in *GATA-1.05* mutant erythroid cells, expression of this globin showed no difference between the ALAS-E-null mutant embryos and wild-type embryos in immunohistochemical analysis. In the ALAS-E-null mutant embryos, no significant increase of apoptotic cells was detected by TUNEL analysis (unpublished observation), suggesting that the decreased number of circulating blood cells in the mutant embryos (Table II) is due to defective proliferation and differentiation of primitive erythroid cells. Thus, heme appears to contribute to the erythroid differentiation program after the commencement of globin production, but not at the progenitor stage.

One simple explanation for the observation is to assume a heme-dependent regulator of erythroid differentiation. In this scenario, the intracellular heme level in erythroid cells becomes very low without ALAS-E, so that the presumptive heme-dependent regulator remains inactive and erythroid progenitors cannot differentiate. To date, a heme-dependent protein kinase was reported to exist in erythroid cells (Chen and London, 1995), and a heme-dependent transcription factor was also found in yeast (Guarente, 1992). Therefore, it is plausible that certain transcription factors and/or signaling molecules serve as the heme-dependent regulators.

Recently a zebrafish ALAS-E mutant (*sau*) was identified (Brownlie *et al.*, 1998). Analysis of that mutant proved the presence of an erythroid-specific ALAS isozyme in the fish (Brownlie *et al.*, 1998), demonstrating phylogenic conservation of the two-isozyme system of ALAS (Yamamoto *et al.*, 1994). The analysis also provided evidence for the importance of ALAS-E in zebrafish hematopoiesis. On the contrary, however, zebrafish ALAS-E appeared to have diverged substantially from the mammalian enzyme in that the *ALAS-E* gene was not located on the X chromosome nor were ring sideroblasts observed in the zebrafish mutant. In addition, since *sau* is a chemically induced mutant containing residual ALAS-E activity, one can not assess the complete lack of ALAS-E activity in the mutant.

This study also revealed the essential contribution of heme to *in vivo* iron metabolism. The TfR pathway has been reported to supply iron for heme biosynthesis in erythroid cells (Ponka, 1997). However, despite the marked decrease of TfR surface expression, iron accumulation proceeded in the ALAS-E mutant primitive erythroid cells, and finally resulted in diffuse cytoplasmic iron accumulation. Thus, the iron import pathway responsible for the diffuse cytoplasmic iron accumulation is either independent of the TfR system or uses the residual TfR efficiently. We have to assume the presence of a hitherto unrecognized TfR-independent cellular iron import system or TfR regulation system in erythroid cells. Importantly, since the iron overload was caused by the lack of ALAS-E, the iron uptake pathway is most likely to be regulated by heme.

Consistent with this notion is the recent observation that TfR-deficient mouse embryos were not anemic until E10.5 (Levy *et al.*, 1999). The TfR mutant embryo eventually developed anemia by E12.5. These observations suggest the presence of another iron uptake pathway, which is independent of the TfR system and can partially sustain the primitive hematopoiesis. In this study, we found that although TfR expression was markedly lower in E9.5 and E10.5 ALAS-E-null embryos, iron accumulation was significant. It is therefore quite plausible that the iron uptake pathway operating in the TfR-deficient primitive erythroid cells is similar to that causing iron overload in ALAS-E knockout mouse embryos. Since TfR was expressed normally in E8.5 ALAS-E-null mutant embryos, down-regulation of TfR expression in E9.5–10.5 embryos is suggested to be due to excess iron exerting negative regulation through the IRE. Another important observation is that heme oxygenase 1-deficient mice showed impaired iron re-utilization (Poss and Tonegawa, 1997). This also supports the essential contribution of heme to the regulation of the iron uptake pathway. Furthermore, several iron metabolism regulator genes were identified recently, such as the hemochromatosis gene *HFE* and the microcytic anemia gene *Nramp2* (reviewed in Andrews and Levy, 1998). It will be of interest to examine the relationship of these regulator genes to cytoplasmic iron accumulation in the ALAS-E-deficient mice.

The site and profile of iron accumulation in the mutant erythroid cells appeared to be distinct from those of ring sideroblasts in XLSA patients. Electron microscopic analysis demonstrated that the mitochondrial iron deposition in mutant erythroid cells was not so strong that it was obscured by the presence of a large amount of cytoplasmic iron. In contrast, only mitochondrial iron deposition (i.e. ring sideroblasts) was observed in the definitive erythroid cells of XLSA patients or in chimeric mice derived from ALAS-E-null mutant ES cells. Thus, the lack of erythroid heme synthesis, provoked by the ALAS-E deficiency, leads to the formation of ring sideroblasts in definitive erythroid cells and to diffuse cytoplasmic iron accumulation in primitive erythroid cells. Elucidation of the molecular mechanism(s) underlying the differences in iron accumulation in primitive and definitive erythroid cells will be one focus of our future research.

Materials and methods

ALAS-E gene targeting

The targeting vector was constructed using the ALAS-E genomic clones as previously described (Harigae *et al.*, 1998). A reversed PGK-Neo cassette replaced the genomic region from the *Sma*I site in exon 8 to the *Stu*I site in exon 9 (Figure 1A). A reversed MC1-HSV-tk cassette was ligated 5′ to the construct. An 11 kbp genomic region from the *Stu*I site in exon 9 to the *Bam*HI site in exon 11 was used as a 3′-homology region. This construct was linearized with *Sal*I and electroporated into E14 ES cells with male karyotype. Colonies resistant to G418 were selected, expanded and analyzed by PCR. A pair of primers (sense, 5′-GAGGCTGCTTCATCCTGTTATACTG-3′; antisense, 5′-AATGG-GCTGACCGCTTCCTCGTGCT-3′), which amplifies a 2.5 kbp genomic fragment composed of part of intron 7/exon 8 and part of the *Neo* gene, was used for the screening. PCR-positive clones were also analyzed by Southern blotting analysis. Positive clones were injected into blastocysts from C57/BL6 mice, which were then transferred to pseudo-pregnant ICR recipient mice. Male mice chimeric for the targeting allele were mated with wild-type female mice (C57/BL6 or Balb/c), and female heterozygous F_1 mice were examined by a PCR analysis that amplified the Neo cassette sequence. We determined the sex of these embryos by using PCR amplification of the Y chromosome-specific *Zfy-1* gene (Koopman *et al.*, 1991). To detect expression of ALAS-E mRNA, RT–PCR analysis was carried out as previously described (Suwabe *et al.*, 1998).

Histological and cytological analyses of embryos

Embryos and adult tissues were fixed in 10% buffered formalin and embedded in paraffin. Sections were stained with benzidine (Pickworth, 1934) or Prussian Blue (McFadzean and Davis, 1948) to examine the presence of hemoglobin and ferric iron, respectively. Sections were counter-stained with Kernechtrot according to the standard procedure. Smears of chimeric mouse blood were fixed with formalin vapor, stained with Prussian Blue and counter-stained with Safranin O (McFadzean and Davis, 1948). Cell surface TfR was stained using alkaline phosphatase-conjugated HANA5 antibody (kindly provided by Dr Tasuo Kina). Smears of blood collected from yolk sacs by needling were fixed and stained with Wright–Giemsa for morphological observation.

Electron microscopy and FACS analysis

Electron microscopic analysis was carried out using standard procedures (Sabatini *et al.*, 1963). For FACS analysis, a single cell suspension of E10.0 yolk sac cells was prepared with a 27 gauge needle. The expression of TfR and TER119 in each sample was analyzed by two-color FACS analysis with fluorescein isothiocyanate (FITC)-conjugated HANA5 (anti-mouse TfR antibody) and allophycocyanin (APC)-conjugated anti-TER119 (Ikuta *et al.*, 1990) antibody, respectively.

Iron quantification by atomic absorption spectrometry

For iron quantification, a single cell suspension of E10.5 was prepared by passing embryo and yolk sac through a 27 gauge needle and then a nylon mesh. The cell pellet was dissolved in nitric acid solution. Atomic absorption spectrometry analysis of the cell solution was performed using a Z-5000 5000-type polarized Zeeman atomic absorption spectrometer.

Colony assay

Yolk sac cells were inoculated into 0.8% methylcellulose and cultured in the presence of erythropoietin (2 U/ml) and stem cell factor (SCF; 50 ng/ml) (Okuyama *et al.*, 1995), and the numbers of colonies (colony-forming unit-erythroid, CFU-E) formed were counted.

Intercross experiment with a reporter transgenic mouse line

Female mice heterozygous for the *ALAS-E* knockout mutation were crossed with transgenic mice homozygous for a pIE3.9-LacZ reporter transgene (Onodera *et al.*, 1997) to generate LacZ-positive embryos harboring the ALAS-E-null mutation [compound mutation designated *ALAS-E (–/Y)::LacZ*]. 5-Bromo-4-chloro-3-indolyl-β-D-galactoside (X-gal) staining was performed as previously reported (Onodera *et al.*, 1997).

Acknowledgements

We thank Drs Tatsuo Kina, Masaki Nakazawa, Priscilla Wilkins Stevens and Naomi Kaneko for help. This work was supported in part by Grants-in-Aid from the Ministry of Education, Science, Sports and Culture; Core Research for Evolutional Science and Technology (CREST); and the Japanese Society for Promotion of Sciences (JSPS).

References

Andrews,N.C. and Levy,J.E. (1998) Iron is hot: an update on the pathophysiology of hemochromatosis. *Blood*, **92**, 1845–1851.

Bessis,M.C. and Breton-Gorius,J. (1962) Iron metabolism in the bone marrow as seen by electron microscopy: a critical review. *Blood*, **19**, 635–663.

Bessis,M.C. and Jensen,W.N. (1965) Sideroblastic anemia, mitochondria and erythroblastic iron. *Br. J. Haematol.*, **11**, 49–51.

Beutler,E. (1990) Hereditary and secondary acquired sideroblastic anemia. In Williams,W.J., Beutler,E., Erslev,A.J. and Lichtman,M.A. (eds), *Hematology.* McGraw-Hill, New York, NY, pp. 554–557.

Bishop,D.F., Henderson,A.S. and Astrin,K.H. (1990) Human δ-aminolevulinate synthase: assignment of the housekeeping gene to 3p21 and the erythroid-specific gene to the X chromosome. *Genomics*, **7**, 207–214.

Brownlie,A., Donovan,A., Pratt,S.J., Paw,B.H., Oates,A.C., Brugnara,C., Witkowska,H.E., Sassa,S. and Zon,L.I. (1998) Positional cloning of

the zebrafish sauternes gene: a model for congenital sideroblastic anaemia. *Nature Genet.*, **20**, 244–250.
Cartwright,G.E. and Deiss,A. (1975) Sideroblasts, siderocytes and sideroblastic anemia. *N. Engl. J. Med.*, **292**, 185–192.
Chen,J.J. and London,I.M. (1995) Regulation of protein synthesis by heme-regulated eIF2α kinase. *Trends Biochem. Sci.*, **20**, 105–108.
Cotter,P.D., Baumann,M. and Bishop,D.F. (1992) Enzymatic defect in X-linked sideroblastic anemia: molecular evidence for erythroid δ-aminolevulinate synthase deficiency. *Proc. Natl Acad. Sci. USA*, **89**, 4028–4032.
Cotter,P.D., May,A., Li,L., Al-Sabah,A.I., Fitzsimons,E.J., Cazzola,M. and Bishop,D.F. (1999) Four new mutations in the erythroid-specific 5-aminolevulinate synthase (ALAS2) gene causing X-linked sideroblastic anemia: increased pyridoxine responsiveness after removal of iron overload by phlebotomy and coinheritance of hereditary hemochromatosis. *Blood*, **93**, 1757–1769.
Cox,T.C., Bawden,M.J., Martin,A. and May,B.K. (1991) Human erythroid 5-aminolevulinate synthase: promoter analysis and identification of an iron-responsive element in the mRNA. *EMBO J.*, **10**, 1891–1902.
Cox,T.C., Bottomley,S.S., Wiley,J.S., Bawden,M.J., Matthews,C.S. and May,B.K. (1994) X-linked pyridoxine-responsive sideroblastic anemia due to a THR388-to-SER substitution in erythroid 5-aminolevulinate synthase. *N. Engl. J. Med.*, **330**, 675–679.
Dandekar,T., Stripecke,R., Gray,N.K., Goossen,B., Constable,A., Johansson,H.E. and Hentze,M.W. (1991) Identification of a novel iron-responsive element in murine and human erythroid δ-aminolevulinic acid synthase mRNA. *EMBO J.*, **10**, 1903–1909.
Fujita,H., Yamamoto,M., Yamagami,T., Hayashi,N. and Sassa,S. (1991) Erythroleukemia differentiation. Distinctive responses of the erythroid-specific and nonspecific δ-aminolevulinate synthase mRNA. *J. Biol. Chem.*, **266**, 17494–17502.
Furuyama,K. *et al*. (1997) Pyridoxine refractory X-linked sideroblastic anemia caused by a point mutation in the erythroid 5-aminolevulinate synthase gene. *Blood*, **90**, 822–830.
Gong,J., Kay,C.J., Barber,M.J. and Ferreira,G.C. (1996) Mutations at a glycine loop in aminolevulinate synthase affect pyridoxal phosphate cofactor binding and catalysis. *Biochemistry*, **35**, 14109–14117.
Guarente,L. (1992) Mechanism and regulation of transcriptional activation in eukaryotes: conserved features from yeasts to humans. In McKnight,S.L. and Yamamoto,K. (eds), *Transcriptional Regulation*. Cold Spring Harbor Laboratory Press, Cold Spring Harbor, NY, pp. 1007–1036.
Harigae,H., Suwabe,N., Weinstock,P.H., Nagai,M., Fujita,H., Yamamoto,M. and Sassa,S. (1998) Deficient heme and globin synthesis in embryonic stem cells lacking the erythroid-specific δ-aminolevulinate synthase gene. *Blood*, **91**, 798–805.
Ikuta,K., Kina,T., MacNeil,I., Uchida,N., Peault,B., Chien,Y.H. and Weissman,I.L. (1990) A developmental switch in thymic lymphocyte maturation potential occurs at the level of hematopoietic stem cells. *Cell*, **62**, 863–874.
Kappas,A., Sassa,S., Galbraith,R.A. and Nordmann,Y. (1989) The porphyrias. In Scriver,C.R., Beaudet,A.L., Sly,W.S. and Valle,D. (eds), *The Metabolic Basis of Inherited Diseases*. McGraw-Hill, New York, NY, pp. 1305–1367.
Koopman,P., Gubbay,J., Vivian,N., Goodfellow,P. and Lovell-Badge,R. (1991) Male development of chromosomally female mice transgenic for Sry. *Nature*, **351**, 117–121.
Lake-Bullock,H. and Dailey,H.A. (1993) Biphasic ordered induction of heme synthesis in differentiating murine erythroleukemia cells: role of erythroid 5-aminolevulinate synthase. *Mol. Cell. Biol.*, **13**, 7122–7132.
Levy,J.E., Jin,O., Fujiwara,Y., Kuo,F. and Andrews,N.C. (1999) Transferrin receptor is necessary for development of erythrocytes and the nervous system. *Nature Genet.*, **21**, 396–399.
McFadzean,A.J.S. and Davis,J.J. (1948) On the nature and significance of the stippling in lead poisoning, with special reference to the effect of splenectomy. *Q. J. Med.*, **18**, 57–73.
Meguro,K., Igarashi,K., Yamamoto,M., Fujita,H. and Sassa,S. (1995) The role of the erythroid-specific δ-aminolevulinate synthase gene expression in erythroid heme synthesis. *Blood*, **86**, 940–948.
Miwa,Y., Atumi,T., Imai,N. and Ikawa,Y. (1991) Primitive erythropoiesis of mouse teratocarcinoma stem cells PCC3/A/1 in serum free medium. *Development*, **111**, 543–549.
Munakata,H., Yamagami,T., Nagai,T., Yamamoto,M. and Hayashi,N. (1993) Purification and structure of rat erythroid-specific δ-aminolevulinate synthase. *J. Biochem.*, **114**, 103–111.
Okuyama,R., Koguma,M., Yanai,N. and Obinata,M. (1995) Bone marrow stromal cells induce myeloid and lymphoid development of the sorted hematopoietic stem cells *in vitro*. *Blood*, **86**, 2590–2597.
Onodera,K., Takahashi,S., Nishimura,S., Ohta,J., Motohashi,H., Yomogida,K., Hayashi,N., Engel,J.D. and Yamamoto,M. (1997) GATA-1 transcription is controlled by distinct regulatory mechanisms during primitive and definitive erythropoiesis. *Proc. Natl Acad. Sci. USA*, **94**, 4487–4492.
Pickworth,F.A. (1934) New method of study of brain capillaries and its application to regional localization of mental disorder. *J. Anat.*, **69**, 62–71.
Ponka,P. (1997) Tissue-specific regulation of iron metabolism and heme synthesis: distinct control mechanisms in erythroid cells. *Blood*, **89**, 1–25.
Poss,K.D. and Tonegawa,S. (1997) Heme oxygenase 1 is required for mammalian iron reutilization. *Proc. Natl Acad. Sci. USA*, **94**, 10919–10924.
Riddle,R.D., Yamamoto,M. and Engel,J.D. (1989) Expression of δ-aminolevulinate synthase in avian cells: separate genes encode erythroid-specific and nonspecific isozymes. *Proc. Natl Acad. Sci USA*, **86**, 792–796.
Sabatini,D.D., Bensch,K. and Barrnett,R.J. (1963) Cytochemistry and electron microscopy: the preservation of cellular ultrastructure and enzymatic activity by aldehyde fixation. *J. Cell Biol.*, **17**, 19–58.
Suwabe,N., Takahashi,S., Nakano,T. and Yamamoto,M. (1998) GATA-1 regulates growth and differentiation of definitive erythroid lineage cells during *in vitro* ES cell differentiation. *Blood*, **92**, 4108–4118.
Takahashi,S., Onodera,K., Motohashi,H., Suwabe,N., Hayashi,N., Yanai,N., Nabeshima,Y. and Yamamoto,M. (1997) Arrest in primitive erythroid cell development caused by promoter-specific disruption of the GATA-1 gene. *J. Biol. Chem.*, **272**, 12611–12615.
Yamamoto,M., Yew,N.S., Federspiel,M., Dodgson,J.B., Hayashi,N. and Engel,J.D. (1985) Isolation of recombinant cDNAs encoding chicken erythroid δ-aminolevulinate synthase. *Proc. Natl Acad. Sci. USA*, **82**, 3702–3706.
Yamamoto,M., Lim,K.C., Nagai,T., Furuyama,K. and Engel,J.D. (1994) Structure and regulation of vertebrate δ-aminolevulinate synthases. In Fujita,H. (ed.), *Regulation of Heme Protein Synthesis*. AlphaMed Press, Dayton, OH, pp. 11–25.

Received July 12, 1999; revised and accepted September 28, 1999